ELSEVIER

Polymer 40 (1999) 1637–1650

polymer

X-ray scattering study of a poly(methacrylic acid) sample as a function of its neutralization degree

Caroline Heitz[a], Michel Rawiso[b], Jeanne François[a,*]

[a]*Laboratoire de Recherche sur les Matériaux Polymères, CNRS, Université de Pau et des Pays de l'Adour, Helioparc, 2 rue du président Angot 64 000, Pau, France*

[b]*Institut Charles Sadron, ULP-CNRS, 6 rue Boussingault, 67083 Strasbourg, Cedex, France*

Received 28 October 1997; revised 16 March 1998; accepted 16 March 1998

Abstract

A sample of poly(methacrylic acid) [PMA] of molecular weight 50 000 was investigated as a function of its degree of neutralization and the concentration in pure water by X-ray scattering. Complementary potentiometric and viscosimetric studies were made in order to determine the range of ionization degree where the conformational transition occurs, and the limits between the dilute and semi-dilute regimes. Light scattering measurements show that filtered solutions of PMA are aggregate free. The scattering curves of the PMA in excess of chlorydric acid exhibit a q^{-3} behaviour in the high q range, which reveals the collapsed conformation of the chain at short distance. For the partially neutralized PMA, the peak of scattering curves, characteristic of the polyelectrolyte character, is shifted towards higher q values when the polymer concentration increases in agreement with the theoretical predictions. When the concentration is fixed, the q value at the peak maximum increases when the charge parameter increases, but a discontinuity appears in the range of the conformational transition.

Keywords: X-ray scattering study; Poly(methacrylic acid); Correlation peak

1. Introduction

Poly(methacrylic acid) [PMA] is a weak polyacid of particular interest because it exhibits a conformational transition upon increasing its ionization degree. A great number of works have been devoted to that phenomenon through several kinds of experimental investigations: potentiometry [1–5]; viscosimetry [1–7]; solubilization of hydrophobic molecules [8–15]; and calorimetry [16]. It is generally described as a change from a compact conformation to an extended [4] coil conformation (globule to coil). Nevertheless, the origin of such a transition is yet poorly understood. Moreover, the assumption of a globule conformation should be associated with a negative second viriel coefficient [2], which is not clearly ascertained by the literature data. Katchalsky and Eisenberg's studies [6] which show a Mark–Houwink law with an exponent of 0.5 and a value of A_2 close to 0 suggested that PMA is in theta conditions in HCl 0.002 M at 30°C. However, Skouri [17] has found that A_2 is a decreasing function of temperature and becomes 0 for $T = 72$°C [17]. This confirms that PMA solutions exhibit a lower critical solution temperature (LCST), as already demonstrated by Eliassaf and Silberberg [18]. Then, temperatures around room temperature would correspond to rather good solvent conditions.

On the other hand, many works were dedicated during these last years to the study of the intermolecular correlations in polyelectrolytes solutions [19–25]. In free salt solutions, the scattering function exhibits a maximum for a scattering vector q^*, whose variations with various parameters, e.g. concentration, charge parameter and ionic strength, were the object of numerous theoretical predictions [26–30]. In the dilute regime, the electrostatic repulsions between the polyions induce the formation of a three-dimensional periodic lattice. q^* of the associated correlation peak is predicted to vary as $c_p^{1/3}$, and to be independent of the charge parameter [26,28]. The system is disordered at extremely high dilution. In the semi-dilute regime, according to the isotropic model [26], the chains overlap without order in the solution and they constitute a temporary network of mesh ξ, as for neutral polymers. Due to the electroneutrality conditions (incompressibility), a correlation peak is observed whose maximum position q^* is proportional to ξ^{-1}. The theoretical predictions are [28]:

$$q^* \propto c_p^{1/2}.\alpha^{1/3} \quad (1)$$

* Corresponding author.

0032-3861/99/$ - see front matter
PII: S0032-3861(98)00252-3

In the concentrated regime, the electrostatic repulsions are completely screened out and the chains can be considered as gaussian. In this case, the complete scattering function has been calculated by several authors, using the mean field approximations. Borue and Erukhimovich [29], and Joanny and Leibler [30] predict a mesophase separation under particular conditions near the theta point, when the attractive dispersions forces are compensated by repulsive electrostatic interactions. In the weak coupling limit, the more or less hydrophobic character of the polyion backbone must be taken into account [30].

A whole set of experimental data obtained on various polyelectrolytes using small angle neutron (SANS) and X-ray (SAXS) scattering, and elastic light scattering (ELS), are in rather good agreement with such predictions [19–25]. Nevertheless, the presence of heterogeneities, often described as the 'extraordinary phase', introduces some confusion in the interpretation of the results [31–36].

The PMA has been extensively studied by scattering methods [37–47]. At low values of α and for concentrations higher than the critical overlap concentration, c_p*, the SANS experiments of Mossaid et al. [46,47] seem to be reasonably consistent with the predictions for the concentrated regime. Plestil and co-workers [41–44] have studied the variations of q* with c_p and α, and made an attempt to characterize the persistence length (SAXS and SANS measurements), and using deuterated PMA chains they have determined the dimensions of the chains. Nevertheless, in these works, the influence of the conformational transition on the scattering functions was never considered.

The aim of the present work is to discuss a series of SAXS experiments performed with a low molecular weight sample of PMA ($M_w = 50\,000$) in pure water in the whole range of α, below and above the transition. Special care will be taken for the calculation of the contrast factor through density data. The experimental conditions are fixed according to the results of potentiometric and viscosimetric studies, which allowed us to determine the transition region as a function of polymer concentration and estimate the overlap concentration c_p*. A static light scattering study was used to evaluate the second viriel coefficient as a function of α and investigate the homogeneity of the solutions.

2. Experimental

2.1. Polymer sample

The PMA sample was prepared by radical polymerization in water at 70°C, using potassium persulfate as initiator and quaternized mercaptoethylbutylamine as transfer agent. The polymer under its acid form was lyophilized. A first purification was carried out by three times precipitation in ether from a solution in methanol. Non-negligible amounts of sulfur (1%), nitrogen (0.3%) and chlore (1%) are still present after this treatment, as measured by elemental analysis. Further purification is achieved by dialysis and ionic exchange (cationic resins from Merck), which reduces the percentage of these elements down to 0.2, 0.09 and 0 respectively, close to the values estimated from the number average molecular weight of the sample and assuming the presence of a mercaptoethylbutylamine at one end of the chain.

The sample was characterized by size exclusion chromatography either in aqueous medium (using a mixture of water/acetonitrile, 80/20 volume per volume and a double detection: refractometry and small angle light scattering detection, Chromatix apparatus) or in tetrahydrofuran (refractometric and multi-angle light scattering detection) after esterification [48]. The weight average molecular weight M_w was found to be 58 000 and 54 000 from the two methods, respectively. The polydispersity index was approximately 2.

2.2. Experimental methods

2.2.1. Potentiometry

The potentiometric titrations were performed using a pH meter Metrhom 605 using a combined glass electrode. The titrant was a NaOH solution (0.1–5 M), according to the polymer concentration. The measurements were made at 20°C under nitrogen, with constant stirring.

2.2.2. Viscosimetry

The viscosity of the polymer solutions was measured with an automatic capillary viscometer of the Gramain–Libeyre type (SEMATECH, Viscologic TI1) using a capillary of 0.56 mm i.d. The apparatus was thermostated at 20°C.

2.2.3. Light scattering

The light scattering experiments were carried out using two different apparatus: a commercial one (SEMATECH) working with a laser source He–Ne of wavelength $\lambda = 6320$ Å and a home-built one equipped with a Ar laser source ($\lambda = 5140$ Å). The scattering angle, θ, range investigated was between 30 and 140°.

We will consider I/Kc_p or its reciprocal, where I is the excess of scattered intensity of the solution with respect to the solvent, corrected by the scattering volume, c_p is the polymer concentration expressed in g/ml and K is the product of the apparatus optical constant by the square of the refractive index increment, dn/dc.

At first, a batch of solution of the sample under its acid form was prepared and gently stirred for one day up to complete solubilization. Then, the pH of the solution was adjusted by adding small aliquots of NaOH solution and the neutralized solutions were then filtered on 0.2 mm filters (Dynagard) directly in the measurement cells.

2.2.4. Refractometry

The measurements of the refractive index increments, dn/dc, were measured with a Brice–Phoenix apparatus.

For the sample under its acid form, dn/dc was determined in pure water, without dialysis, for the partially neutralized sample, it was measured in solution containing 0.05 M NaCl

after dialysis equilibrium. The variation of dn/dc versus α was found to be:

$$\frac{dn}{dc} = 0.171 + 0.092\alpha \text{ (ml/g)} \quad (2)$$

for $\lambda = 4880$ Å.

2.2.5. Small angle X-ray scattering

The SAXS experiments were made at the LURE laboratory using two different apparatus D22 and D24.

On D22, the wavelength was set at 1.38 Å, the sample-detector distance D was 0.923 m and the range of scattering vector was $0.005 < q < 0.25$ Å^{-1}. The transmission measurements are made simultaneously with the scattering measurements, using scintillators put after and before the sample, and perpendicularly to the incident beam.

On D24, we used a wavelength $\lambda = 1.488$ Å, $D = 0.875$ and 2.003 m which allow us to cover the q ranges: $0.02 < q < 0.45$ Å^{-1}, and $0.005 < q < 0.16$ Å^{-1}, respectively. The transmission measurements were made using a carbon black sheet automatically put in the beam between the sample and detector, for a short time at the beginning and end of each measurement run.

The total scattered intensity $I_{tot}(i)$ registered in channel i, after normation to the incident intensity I_0, is given by [49]:

$$I_{tot}(i) = I_{sam}(i) * Tr(\text{CB}) + I_{CB}(i) * Tr(\text{sam}) \quad (3)$$

where I_{sam} and I_{CB} are the intensities scattered by the sample alone and the carbon black alone, respectively. Tr(sam) and Tr(CB) are transmissions of the sample and the carbon black. The transmission of the sample can be calculated from:

$$Tr(\text{sam}) = \frac{\sum_i I_{tot}(i) - Tr(\text{CB}) * \sum_i I_{sam}(i)}{\sum_i I_{CB}(i)} \quad (4)$$

When the term Tr(CB)*$I_{sam}(i)$ is low, one can make the following approximation:

$$Tr(\text{sam}) = \frac{\sum_i I_{tot}(i)}{\sum_i I_{CB}(i)} \quad (5)$$

With both apparatus, the excess of scattered intensity I of the solution with respect to the solvent is obtained from:

$$I = \left(\frac{I_{sam}(q)}{Tr(\text{sam})} - \frac{I_{ec}(q)}{Tr(\text{ec})}\right) - \phi_v^{solv}\left(\frac{I_{solv}(q)}{Tr(\text{solv})} - \frac{I_{ec}(q)}{Tr(\text{ec})}\right) \quad (6)$$

where the ec index corresponds to the empty cell, solv index corresponds to the cell filled by the solvent, ϕ_v^{solv} is the volume fraction of the solvent.

3. Results

3.1. Poly(methacrylic acid) in HCl solution

3.1.1. Light scattering

We have studied by light scattering the PMA sample in a solution of HCl, 0.1 M. Under these conditions, the average ionization of the carboxylate groups is 10^{-4} (taking $pK_a = 5$) which corresponds to less than 0.1 charge per chain. The experiments were performed for concentrations comprised between $2*10^{-3}$ and $4*10^{-2}$ g/ml, and as expected for the relatively low molecular weight of the sample, no angular dysymmetry and no small angle excess of scattered intensity were observed. Moreover, the molecular weight obtained by extrapolation at zero concentration is 54 000, a value in excellent agreement with that obtained by SEC. This shows that the aqueous solutions of uncharged PMA contain no aggregates or a negligible amount of them.

Fig. 1 shows that the second viriel coefficient is positive and a value of $A_2 = 1.46*10^{-4}$ mole.ml.g^{-2} was found.

3.1.2. SAXS

An HCl solution of PMA ($4.6*10^{-2}$ g/ml) was studied by X-ray scattering using the D24 instrument and the scattering curve is represented in Fig. 2*a*. It does not exhibit a maximum, which confirms the absence of charges along the chain. In a first attempt to get an approximate value of the radius of gyration, we have used a Zimm representation and neglected the second viriel coefficient: a value $R_G = 50$ Å was found, meaning that the q range explored does not correspond to the Guinier range ($qR_g < 1$). In order to precisely obtain the R_G value, and extract the form factor $P(q)$ of the macromolecule, we have used the following procedure. The classical Zimm formula can be written:

$$\frac{1}{I(q)} = \frac{1}{AK_x^2}\frac{m^2}{c_p N_{av}}\left(\frac{1}{M_w}P^{-1}(q) + 2A_2c_p\right) \quad (7)$$

where m is the molecular weight of the monomer unit, N_{av} the Avogadro number, A the apparatus constant and K_x^2 the contrast factor.

Moreover, for $qR_G < 3$, $P(q)$ is closed to the Debye function $P_D(q)$. For a polydispersed sample, assuming a Schultz–Zimm distribution, $P_D(q)$ is given by [50]:

$$P_D(x) = \frac{2[x - 1 + (1+ux)^{-1/u}]}{(1+u)x^2} \quad (8)$$

with

$$x = \frac{q^2 < R_G^2 >_z}{1+2u} = \frac{q^2 < R_G^2 >_w}{1+u} \quad (9)$$

and

$$u = \frac{M_w}{M_N} - 1 \quad (10)$$

The fit of the experimental scattering function by Eq. (7) and Eq. (8), in the range $qR_G < 3$, allows us to determine the

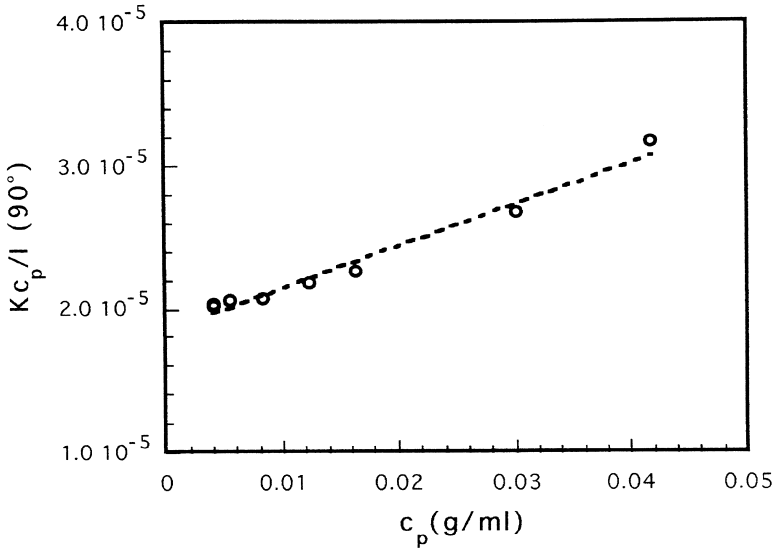

Fig. 1. Light scattering experiment on PMA in HCl, 0.1 M solution: plot of $(Kc_p/I)_{\theta=90^\circ}$ versus c_p.

values of $A^*K_x^2$ and the weight average radius of gyration $< R_G^2 >_w^{1/2}$. A value of $< R_G^2 >_w^{1/2} = 53$ Å was found. In the whole range of q, the $P(q)$ function is then obtained from Eq. (7). In Fig. 2*b*, the $q^2P(q)$ function is plotted *versus* q.

Up to now, the conformation of uncharged PMA has not been clearly elucidated. Firstly, one may consider the value of R_G and compare it to that expected either for a compact sphere or for a gaussian coil. A value of $< R_G^2 >_w^{1/2} = 53$ Å should correspond to a sphere of radius = 68 Å, much

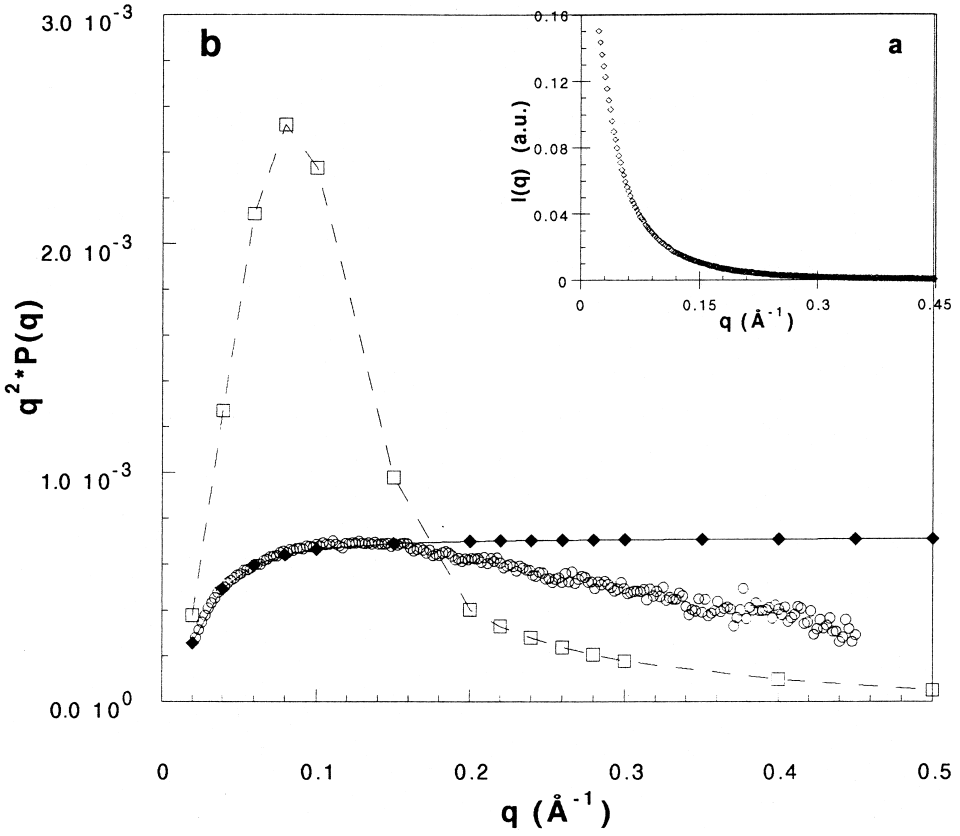

Fig. 2. X-ray scattering experiment on PMA in HCl, 0.1 M solution, $c_p = 4.6 \times 10^{-2}$ g/ml. (a) Scattering function $I(q) = f(q)$; (b) plot of $q^{2*}P(q)$ [$P(q)$ calculated as explained in the text] *versus* q (○); and $q^{2*}P(q)$ calculated for a gaussian coil (◆) and a sphere (□).

higher than the value $R = 24$ Å, calculated from

$$R = \sqrt[3]{\frac{M_w.v_{sp}.10^{24}}{N_{av}}\frac{3}{4\pi}}$$

where v_{sp} is the specific volume of PMA = 0.68 ml/g [51]. On the other hand, many vinyl polymers [polystyrene, poly(methylmethacrylate), polyacrylamide] have in theta and in good solvents approximately the same dimensions for the same polymerization degree N. For instance, the N dependence of the radius of gyration for polyacrylamide in theta conditions is $R_G = 3.3\ N^{0.5}$ [52] which leads to $R_G =$ 79 Å for our PMA sample ($N = 581$), a value higher than the experimental one. Then, the neutral PMA dimensions seem to be intermediate between those of a compact coil and a gaussian coil.

In Fig. 2*a*, the $q^2P(q)$ functions for systems of polydisperse spheres and gaussian coils can be compared with those deduced from the data treatment described above. The form factor of a sphere and a gaussian coil are given by:

$$P_{sph}(q) = \left[\frac{3}{x^3}(\sin x - x\cos x)\right]^2 \quad \text{with } x = qR = q * 24 \tag{11}$$

and

$$P_D(q) = \frac{2}{x^4}(\exp(-x^2) + x^2 - 1)$$

$$\text{with } x = q < R_G^2 >^{1/2} = q * 53 \tag{12}$$

respectively, and we used the molecular weight distribution function of Schultz–Zimm, with $\frac{M_w}{M_n} = 2$:

$$w(M) = \frac{4M}{M_w^2}\exp\left(-\frac{2M}{M_w^2}\right) \tag{13}$$

The experimental form factor strongly differs from that of a sphere, while it diverges from that of a gaussian coil in the high q range only, which makes our initial assumption valid. An approximate q^{-3} dependence of $P(q)$ is observed ($q >$ 0.2 Å^{-1}), while a q^{-1} behaviour is expected due to the local rigidity of the chain. Rawiso et al. [53] have demonstrated that such a divergence can be due to an effect of the chain cross-section. In particular, for q values higher than $1/2L_p$, where L_p is the persistence length of the chains, the q^{-1} dependence of the scattered intensity cannot be obtained when the chain section R_c is close to L_p [54]. It was shown that the form factor must be written:

$$P(q) = P_0(q)\exp\left(-\frac{q^2R_c^2}{2}\right) \tag{14}$$

where $P_0(q)$ is the form factor of the persistence length chain. The variation of $\ln(qP(q))$ *versus* q^2 must be linear in the high q range and the slope gives the value of R_c. Results of Fig. 3, curve a, lead to $R_c = 3.9$ Å. Then, the $P_0(q)$ function can be calculated from Eq. (14), and in the Holtzer's representation, the plot of $q^2M_w/m\ P_0(q)$ *versus* q must tend, for $qL_p > 3.5$ to a plateau whose height gives the

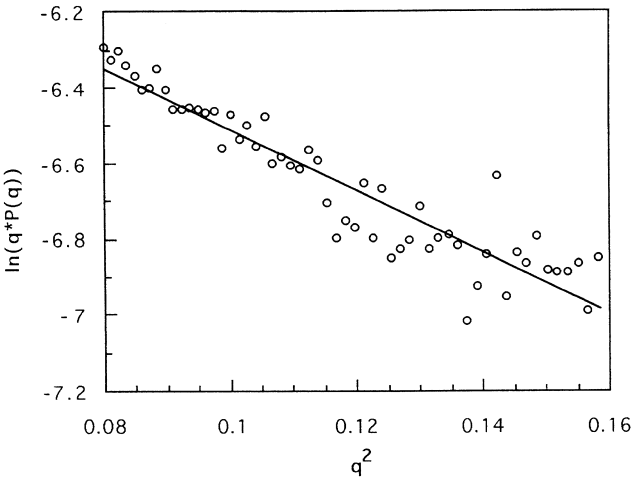

Fig. 3. X-ray scattering experiment on PMA in HCl, 0.1 M solution, $c_p = 4.6 \times 10^{-2}$ g/ml. Plots of (a) $\ln(q*P(q))$ *versus* q^2 and (b) $q^2M_w/mP_0(q)$ *versus* q.

mass per length unit, M_l. The value of L_p found using this method is 12 Å, which seems reasonable for such a polymer, but that of $M_L = 53$ g/Å is much higher than that expected for the PMA molecule $M_L = 34.4$ Å. On an other hand, the radius of gyration of a chain with a persistence length = 12 Å can be calculated using the Benoit–Doty formula [54]:

$$R_g^2 = L^2\left[\frac{L_p}{3L} - \frac{L_p^2}{L^2} + \frac{2L_p^3}{L^3} - \frac{2L_p^4}{L^4}\left(1 - \exp\left(-\left(\frac{L}{L_p}\right)\right)\right)\right] \tag{15}$$

The obtained value of 72 Å is much higher than the experimental one. Finally, the persistence length chain model does not lead to a consistent set of data and cannot explain the divergence between the experimental $q^2P(q)$ function and that of a gaussian particle. Several other models were checked, among which that of a bead necklace close to the description given by Dobrynin et al. [55] for polyelectrolytes in bad solvent. We consider a gaussian chain of N_p adjacent beads of diameter D, each of them containing n_p monomers. The form factor is given by

$$P(q) = P_{sph}\left(q; \frac{D}{2}\right).P_D(q; N_p, D) \tag{16}$$

where $P_{sph}\left(q; \frac{D}{2}\right)$ is the form factor of a sphere of radius $D/2$ [Eq. (11)] and $P_D(q; N_p, D)$ is the form factor of a gaussian coil [Eq. (8) Eq. (9) Eq. (10)] of radius of gyration

$$R_G = \left(\frac{N_pD^2}{6}\right)^{1/2}.$$

The best fit of the experimental results with Eq. (16) is obtained with: $D = 12.6$ Å, $N_p = 102$ and $n_p = 6$.

Fig. 4 shows that this model does not fit the high angle behaviour very well in the Kratky representation. Nevertheless, it is clear that the conformation of the uncharged PMA

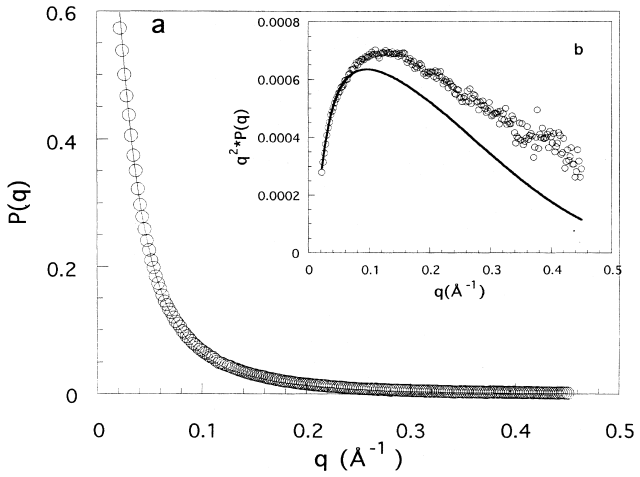

Fig. 4. X-ray scattering experiment on PMA in HCl, 0.1 M solution, $c_p = 4.6 \times 10^{-2}$ g/ml. Fit of the experimental $P(q)$ function (○) with the necklace beads model (full line) in the $P(q) = f(q)$ (a) and in the Kratky (b) representations.

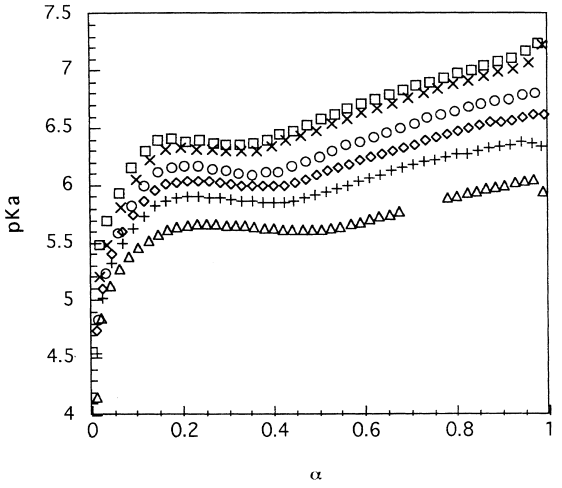

Fig. 5. Potentiometric titration of PMA $pK_a = f(\alpha)$ curves for various values of $c_{pM} = 0.00834$ M (□), 0.02 M (x), 0.0673 M (○), 0.106 M (◇), 0.208 M (+), 0.57 M (△).

is intermediate between that of a compact sphere and a gaussian coil. Its statistics differ at short distance from that of any simple model of a coil, and this suggests that some local folding occurs which is not taken into account by a simple cross-section effect. By considering the presence of helicoïdal residues in the syndiotactic poly(methyl methacrylate) in solution, as well documented in the works of Kirste [56,57], one may suggest that the syndiotactic sequences of the PMA also form such a local helicoïdal conformation. Muroga et al. [45] have also proposed a model with curvature persistence for the syndiotactic PMA, in order to explain the oscillations in the X-ray intensity curves. We assume that the average cross-section of the chain is not a constant but may vary with the local stereochemistry of the polymer.

3.2. Poly(methacrylic acid) as a function of the neutralization degree

3.2.1. Potentiometry

In this part, a is the degree of dissociation calculated by taking into account the auto-ionization of the polyacid at low values of the neutralization ratio.

While the pK_a of a weak polyacid, e.g. PAA, increases monotonously with α, it is well known that the $pK_a = f(\alpha)$ curve for PMA exhibits a discontinuity, as represented in Fig. 5. The pK_a variation is very high in the low α range, then pK_a passes through a maximum at α_1 and a minimum at α_2, and in the last part of the curves, pK_a increases again. This phenomenon was extensively studied in the past, but there is a lack of data concerning the influence of the polymer concentration on this effect. Fig. 5 shows that the discontinuity is observed up to $c_{pM} = 0.57$ M of carboxylate groups. By fitting separately the experimental pK_a values, in the $\alpha < \alpha_1$ and $\alpha > \alpha_2$ ranges, by a second order polynome as proposed by Mandel [58], one can obtain the values of pK_{a0}, corresponding to the dissociation constant of the uncharged polymer. pK_{a0} was found to decrease when c_p increases, for both set of curves, in agreement with other experimental results [59]. Several theories using coil [60,61] or rod [62–64] models were developed to evaluate the α dependence of ΔpK_a:

$$\Delta p\mathrm{Ka} = p\mathrm{Ka} - p\mathrm{K}_0 = 0.434\frac{\Delta G_{el}}{kT} \tag{17}$$

where ΔG_{el} is an electrostatic free energy term which takes into account the work necessary to extract a proton from a uniformly charged polyion. If pK_{a0} is known, it should be possible to compare the experimental and theoretical predictions, and draw some conclusions on the conformation of the uncharged PMA and the nature of the conformational transition. In another work [66], we have tried to make these confrontations, and found that both models may be compatible with our experimental results. In the coil model, the radius should increase from 115 Å at $\alpha = \alpha_1$ to 160 Å at $\alpha = \alpha_2$, and in the rod-like model, the diameter of the charged cylinder should be twice as high in the region $\alpha < \alpha_1$ than in the region $\alpha > \alpha_2$. Then the potentiometric titration results do not allow us to definitely conclude on the nature of the transition and, moreover, the uncertainties on the pK_{a0} values and its variation with the polymer concentration make such a confrontation doubtful. What must be kept in mind is the fact that even at relatively large c_p values, when the long distance interactions are screened out, the polymer exhibits a transition and this means that only local conformation changes are implied in this transition. In this respect, the second model of a rod of variable diameter seems more realistic than a coil model, although the overall dimensions of the uncharged polymer are close to those of a slightly collapsed coil.

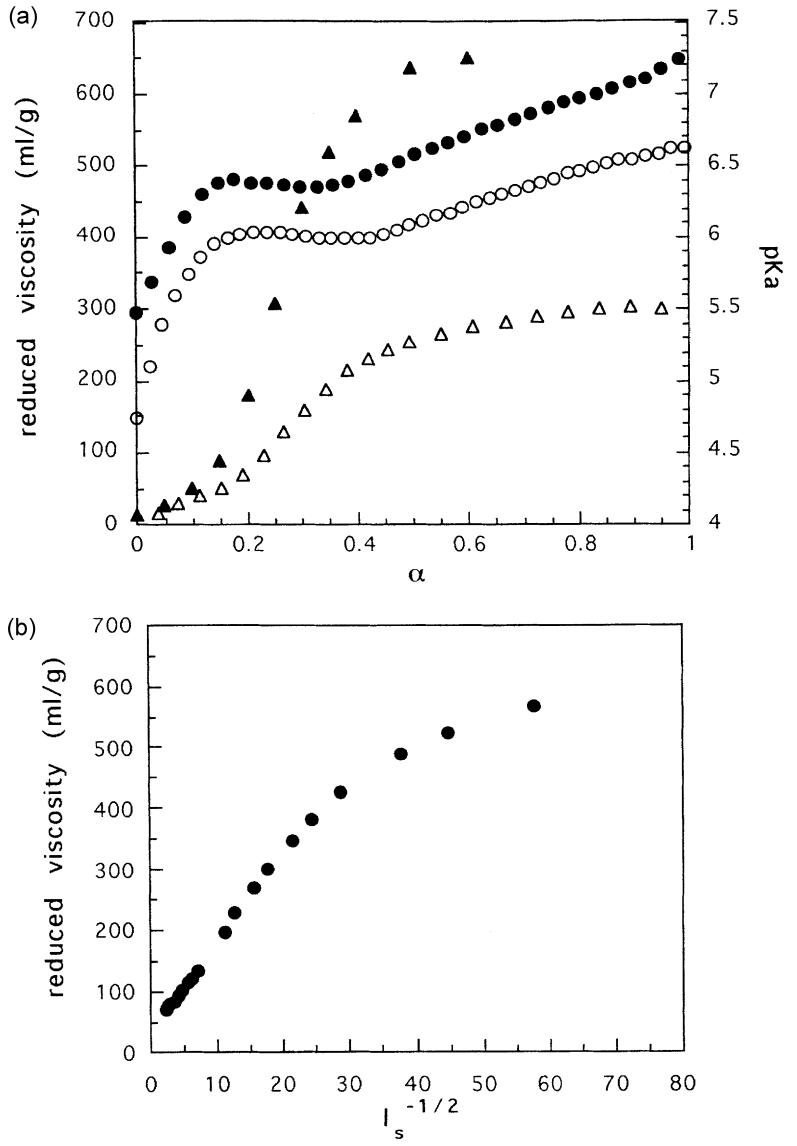

Fig. 6. Reduced viscosity η_{red} of PMA. (a) Plot of pK_a (circles) and η_{red} (triangles) versus α: $c_p = 6.88 \times 10^{-4}$ g/ml (full symbols), $c_p = 9.03 \times 10^{-3}$ g/ml (open symbols). (b) Plot of η_{red} *versus* $I_s^{-1/2}$; $c_p = 6.88 \times 10^{-4}$ g/ml.

3.2.2. Viscosity

Fig. 6*a* compares the variation of pK_a and that of the reduced viscosity η_{red} with α at two polymer concentrations. This result confirms that the discontinuity in the pK_a curves corresponds to an abrupt increase of η_{red}. On the other hand, we have also measured η_{red} for $c_p = 6.88 \times 10^{-4}$ g/ml at $\alpha = 0.75$ as a function of the salinity c_s (NaCl) and obtained a linear variation of $\eta_{red} = f(c_s^{-1/2})$ for $c_s^{-1/2} < 30$. In Fig. 6*b*, c_p is low enough to consider that the intrinsic viscosity $[\eta]$ is very close to η_{red}. The aim of this viscosimetric study was in fact to evaluate the limit between the dilute and semi-dilute regime for our PMA samples in pure water, such information being necessary for interpreting the X-ray scattering results presented below. The classical definition of the c_p*, the overlap critical concentration of polymers, is given by

$$c_p^* = \frac{M}{N_a \frac{4}{3}\pi R_g^3} \tag{18}$$

but may be also evaluated through:

$$c_p^{**} = \frac{1}{[\eta]} \tag{19}$$

For the uncharged PMA, relation (18) can be used, since R_G is known, one finds $c_p^* = 0.16$ g/ml.

In the case of salt-free polyelectrolyte solution, the difficulty in the determination of c_p* or c_p** arises from the variation of R_G with concentration. In the case of acrylamide/acrylic acid copolymers, Boudenne and François [24] have proposed a graphical method to avoid this difficulty,

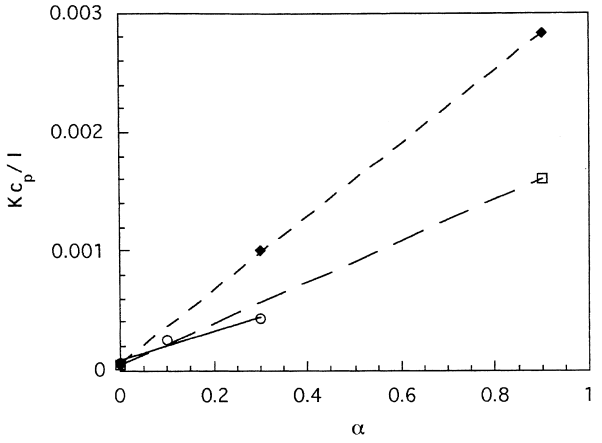

Fig. 7. Light scattering experiment of PMA in pure water: plot of Kc_p/I *versus* α for different concentrations: $c_p = 6.88*10^{-4}$ g/ml (○), $c_p = 9.03*10^{-3}$ g/ml (□), $c_p = 4.14*10^{-2}$ g/ml (♦).

using the known ionic strength (I_s) dependence of R_G. We will use the same approach in our case, making the hypothesis according to which η_{red} varies with I_s, as shown in Fig. 6*b*, even in the absence of salt. I_s is expressed as:

$$I_s = c_s + \tfrac{1}{2}\alpha c_{pM} \text{ or } I_s = c_s + \tfrac{1}{2}0.36c_{pM} \quad (20)$$

under and above the value of α corresponding to the Manning condensation threshold, respectively. Then, one can calculate I_s for each polymer concentration and evaluate $[\eta]$ from the results of Fig. 6*b*.

One finds, for $\alpha = 0.75$: $c_p{}^{**} = 1.3 \times 10^{-2}$ g/ml for $c_p = 4.3 \times 10^{-2}$ g/ml, and $c_p{}^{**} = 7.5 \times 10^{-3}$ g/ml for $c_p = 9 \times 10^{-3}$ g/ml, which means that the higher c_p corresponds to the semi-dilute regime and the lower one to the limit between the dilute and semi-dilute regimes.

3.2.3. Static light scattering

By using the method of purification of the solution by filtration, we never obtained dysymmetry in the scattered intensity, which shows the absence of aggregates, in the whole range of α. As expected for a polyelectrolyte, the scattered intensity decreases when α increases and tends, for $\alpha \rightarrow 1$, towards values very small and difficult to measure with a good accuracy. In the presence of salt, the mean field approximation leads to the following expression for the variation of I *versus* c_p and q:

$$\frac{I}{Kc_pM_w} = \frac{P(q)}{1 + \left(2A_2 + \dfrac{4\pi l_b \alpha^2 N_a}{m^2(q^2+\kappa^2)}\right)c_pM_wP(q)} \quad (21)$$

where $\kappa^2 = 4\pi l_b N_{av} I_s$ (κ^{-1} is the Debye length and l_b the Bjerrum length). At $q = 0$ and if A_2 can be neglected, Eq. (21) is reduced to:

$$\left(\frac{Kc_p}{I} - \frac{1}{M_w}\right)_{q=0} \propto \alpha \quad (22)$$

Fig. 7 shows that straight lines are obtained whose slope increases when c_p increases. Moreover, by taking into account the non-electrostatic viriel A_2, in Eq. (21), it is possible to determine from experimental results the electrostatic term $A_{2_{el}}$ which should be equal to $4\pi l_b \alpha^2/m^2\kappa^2$. As shown in Table 1, the experimental values are much lower than the calculated ones, and the difference decreases when α and c_p increase. Such a mean field approximation is only valid for the concentrated regime and highly interpenetrated coils, and when the chain statistics are gaussian, which is not the case of our experimental conditions.

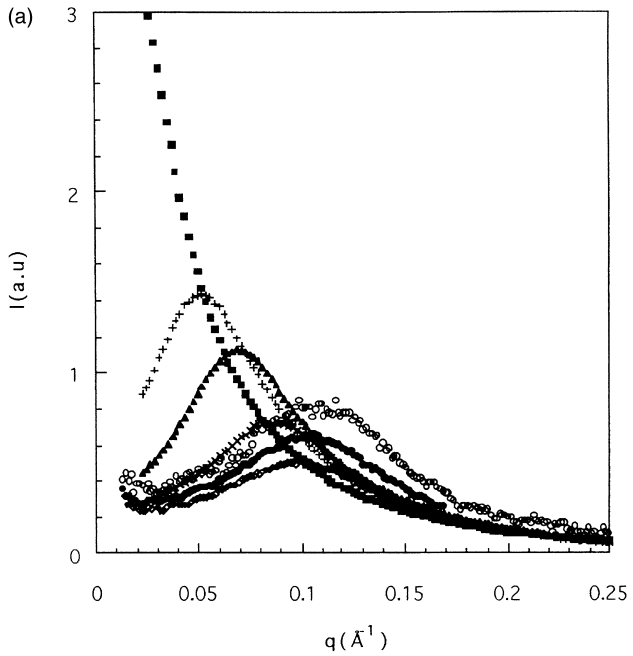

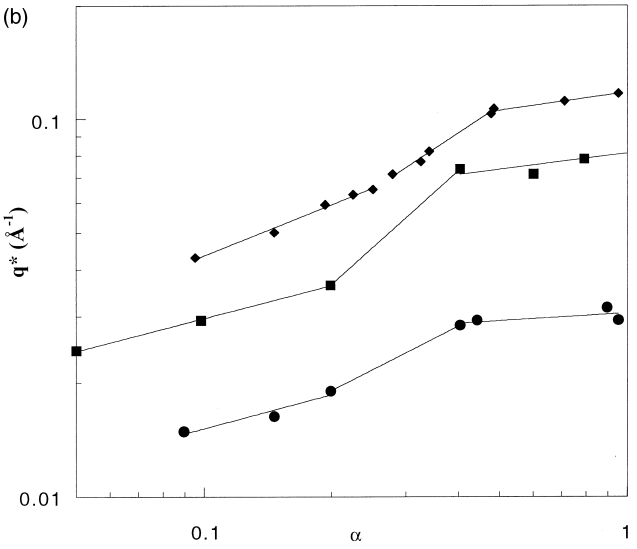

Fig. 8. (a) X-ray scattering experiment on PMA in pure water; $c_p = 0.046$ g/ml for different values of α: $\alpha = 0$ (■), $\alpha = 0.05$ (+), $\alpha = 0.15$ (▲), $\alpha = 0.32$ (x), $\alpha = 0.48$ (♦), $\alpha = 0.71$ (⊙), $\alpha = 0.95$ (○). (b) Logarithmic plot of q^* versus α. ♦, $c_p = 0.045$ g/ml; ●, $c_p = 0.009$ g/ml; ■, $c_p = 0.033$ g/ml. Results of Ref. [42].

3.2.4. X-ray scattering

The PMA solutions were studied on D22 and D24 instruments for $0 < \alpha < 1$ and $0.01 < c_p < 0.15$ g/ml.

3.2.4.1. Influence of the degree of neutralization. Fig. 8*a* shows examples of scattering curves obtained for the same polymer concentration and for various degrees of neutralization (the scattered intensities are not normalized to the contrast factor). The scattering peak appears for α as low as 0.05 and is shifted towards higher q values when α increases. q^* is plotted versus α for two concentrations studied in this work and the results of Plestil et al. [42] obtained for another c_p value are also reported for comparison (Fig. 8*b*). Both sets of data show a discontinuity in the curves, which exhibit three different parts:

1. $\alpha < 0.2$, which corresponds to the existence of the compact conformation, the following power laws are obtained:

$$c_p = 0.045 \text{ g/ml } q* \approx \alpha^{0.26} \quad (23)$$

$$c_p = 0.0090 \text{ g/ml } q* \approx \alpha^{0.15} \quad (24)$$

The exponents of such laws are intermediate between those expected for the dilute and semi-dilute regimes. For the lower concentration, which corresponds surely to the dilute range, q^* is almost independent of α, as predicted by the theories. For the higher one, the exponent is close to that expected for the isotropic model. This is not inconsistent with the viscosity results which suggest that this concentration belongs to the cross-over between the two regimes.

2. $0.2 < \alpha' < 0.5$, range of the transition according to the viscosity and potentiometry studies, q^* increases much more with α. We attribute this behaviour to the conformational change. Indeed, the scattered function is related to the intermolecular correlation and intramolecular ones, as well. If the form factor of the particles abruptly changes, the position of the peak will not only reveal the variation of the intermolecular correlations with α. The influence of the transition on the evolution of the scattering functions was never clearly indicated in the previous works. However, the results of Plestil et al. [43,44] are in excellent agreement with ours, and also reveal the same phenomenon.

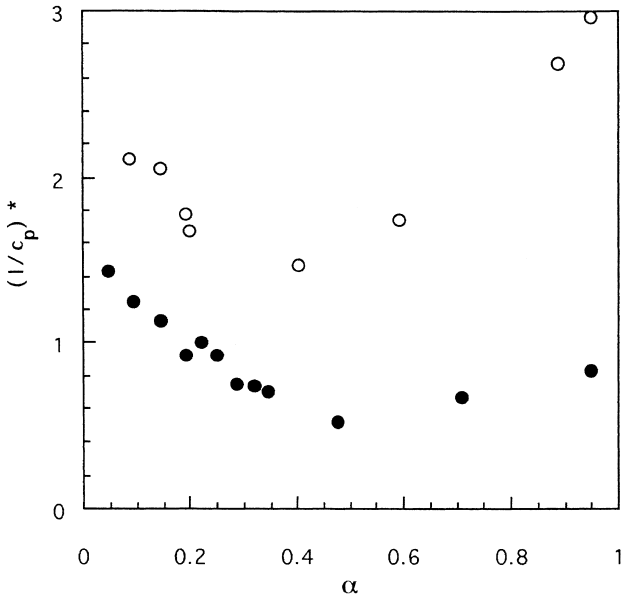

Fig. 9. X-ray scattering experiments on PMA in pure water: variation of the intensity at q^*, $(I/c_p)^*$ *versus* α; $c_p = 0.045$ g/ml: full symbols; $c_p = 0.0088$ g/ml: open symbols.

3. $\alpha' > 0.5$, in this range, q^* varies very little with α. This can be ascribed to Manning [67] condensation.

Fig. 9*a* shows the variation with α of the intensity at q^*, I^*, for two different polymer concentrations. The curves exhibit a minimum at an α value of about 0.5, while a continuous decrease and plateau are expected before and after the Manning threshold, respectively. Such a behaviour was already observed by Plestil et al. [43,44] in their X-rays scattering studies, and these authors have shown that in neutron scattering, I^* decreases as qualitatively expected. An hydration effect was invoked to explain the difference between the X-rays and neutron scattering results. Nevertheless, we whould like to show that it may also be explained by taking into account the variation of specific volume of PMA with α and the Manning condensation, above α_M.

We have calculated the contrast factor by considering the scattering particle as a copolymer constituted by:

1. ionized (COO^-, fraction α) and acid units (COOH, fraction $1 - \alpha$) for $\alpha < \alpha_M$;

Table 1

c_p (g/ml)	α	κ^2 (Å^{-2})	$A_{2_{ell}}$ (mol cm^{3}g^{-2})	$A_{2_{ell}}$ Σ(exp)(mol cm^{3}g^{-2})
$6.88*10^{-4}$	0.020	$8.65*10^{-6}$	0.34	0.0443
	0.1	$4.33*10^{-5}$	1.69	0.337
	0.3	$1.30*10^{-4}$	5.06	0.59
$9.03*10^{-3}$	0.0131	$7.44*10^{-5}$	0.0168	0.00263
	0.9	$5.11*10^{-3}$	0.116	0.176
$4.14*10^{-2}$	0.011	$2.87*10^{-4}$	0.00308	0.00043
	0.3	$7.82*10^{-3}$	0.084	0.0234
	0.9	$23.46*10^{-3}$	0.252	0.0678

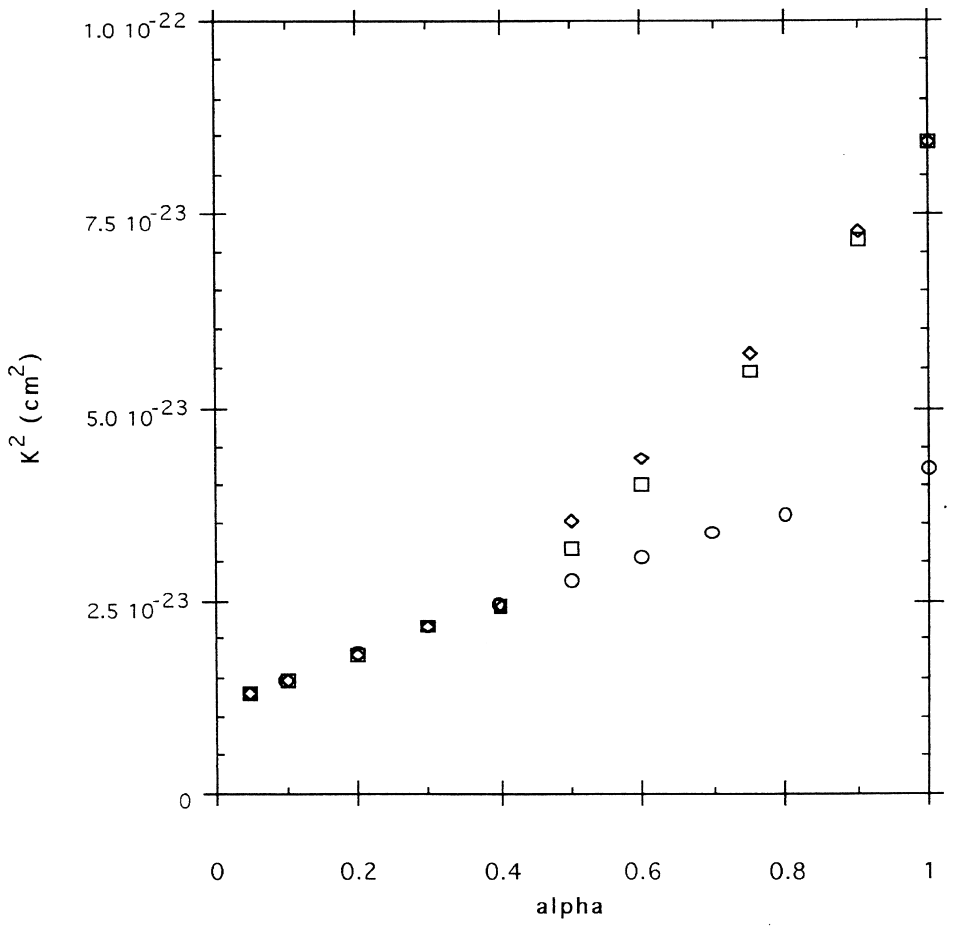

Fig. 10. Variation of the X-ray contrast factor *versus* α: values calculated neglecting Manning condensation (○), taking into account Manning condensation, and using $v_{COOH} = 59.3$ ml/mole [51] (◇) or $v_{COOH} = 55$ ml/mole (see text).

2. (COO^-, fraction α_M), (COOH, fraction $1 - \alpha$) and (COONa units, fraction $\alpha - \alpha_M$) for $\alpha > \alpha_M$.

The average scattering length ,K_x, is:

$$K_x = (1-\alpha)K_{COOH} + \alpha K_{COO-} \quad \text{for } \alpha < \alpha_M \tag{25}$$

$$K_x = (1-\alpha)K_{COOH} + \alpha_M K_{COO-} + (\alpha - \alpha_M)K_{COONa}$$

$$\text{for } \alpha > \alpha_M \tag{26}$$

where K_i for each monomer of type i is expressed by

$$K_i = \frac{v_i}{N_{av}}(\rho_i - \rho_s) \tag{27}$$

ρ_i is the scattering length density:

$$\rho_i = 0.282 \times 10^{-12}\ \frac{Z_i N_{av}}{v_i}$$

where Z_i is the number of electrons of the scattered, v_i its partial molar volume. ρ_s is the scattering length density of the solvent, assumed to contain water and counter ions, which can be calculated from:

$$\rho_s = \frac{\alpha.v_{Na+}.c_{pM}}{1000}\rho_{Na+} + \left(1 - \frac{\alpha.v_{Na} + .c_{pM}}{1000}\right)\rho_{H_2O}$$

$$\text{for } \alpha < \alpha_M \tag{28}$$

$$\rho_s = \frac{\alpha_M.v_{Na+}.c_{pM}}{1000}\rho_{Na+} + \left(1 - \frac{\alpha_M.v_{Na} + .c_{pM}}{1000}\right)\rho_{H_2O}$$

$$\text{for } \alpha > \alpha_M \tag{29}$$

ρ_{H_2O} and ρ_{Na+} are the scattering length density of water and sodium ion, respectively, and v_{Na+} is the partial molar volume of Na^+.

It can be shown that Eq. (25) can be rewritten:

$$K_x = \frac{v_{PMA}}{N_{av}}\left(\frac{0.28210^{-12}ZN_{av}}{v_{PMA}} - \rho_s\right) \tag{30}$$

where

$$v_{PMA} = v_{ex} - \alpha v_{Na+} \tag{31}$$

v_{ex} is the value of the partial molar volume of the partially neutralized PMA including counter ions. We have used the data of Yamashita and Kwak [68].

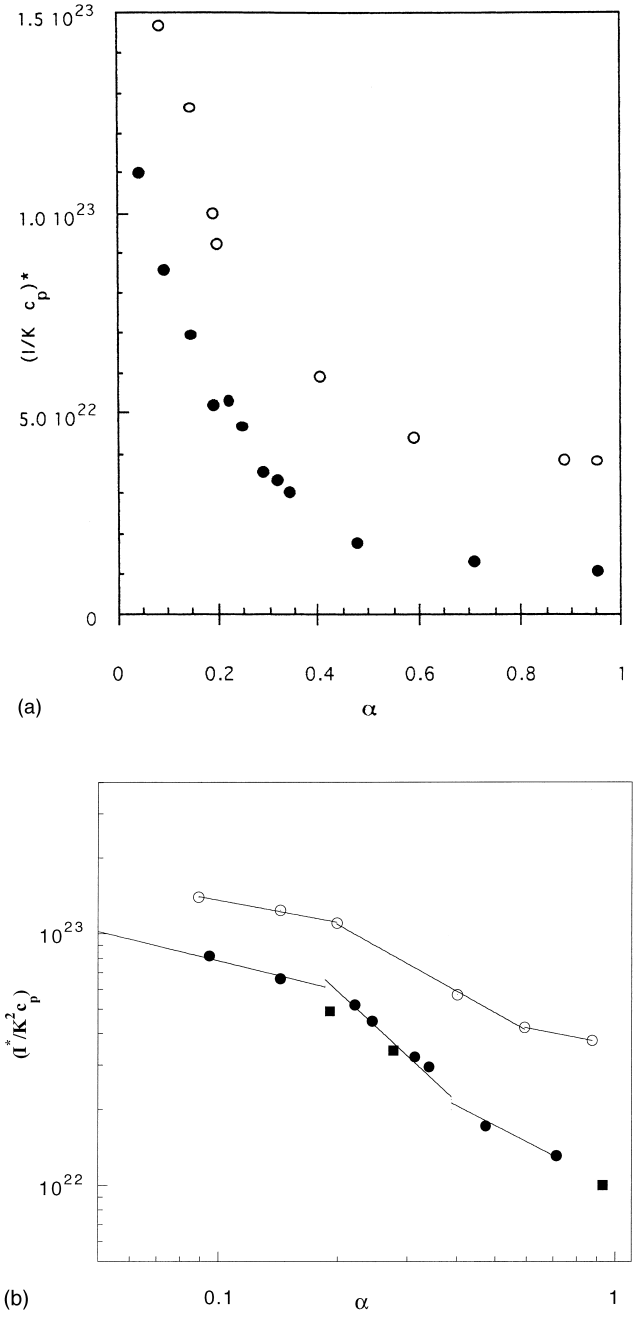

Fig. 11. (a) X-ray scattering experiments on PMA in pure water: variation of $(I/K_x c_p)^*$ *versus* α; $c_p = 0.045$ g/ml: full symbols; $c_p = 0.0088$ g/ml: open symbols. (b) Logarithmic plot of $(I^*/K^2 c_p)$ versus α. ●, $c_p = 0.046$ g/ml; ■, $c_p = 0.044$ g/ml; ○, $c_p = 0.009$ g/ml.

In a first step, for $\alpha > \alpha_M$, v_{COOH} and v_{COO-} were taken as equal to 59.3 and 37.5 ml/mole, respectively, from Tondre and Zana [51]. v_{COONa} was deduced from the results of Ref. [67] (for $\alpha = 1$) and 50, by using the relation:

$$v_{COONa} = \frac{v_{ex} - \alpha_M v_{Na+} - \alpha_M v_{COO-}}{1 - \alpha_M} \tag{32}$$

Nevertheless, some problem arises from the value of v_{COOH} which was determined by Tondre and Zana [51] at $a = 0$ before the conformational transition. It is not clear whether the specific volume of the COOH monomer units remains the same after the transition. Assuming that the value of v_{COO-} is correct, a new average value of v_{COOH} (= 55 ml/mole) can be calculated from the literature data, using relation (25).

Fig. 10 shows that K_x^2 continuously increases with α, when the Manning condensation is neglected, while the curve presents a discontinuity at $\alpha = \alpha_M$ with a higher slope for $\alpha > \alpha_M$ than for $\alpha < \alpha_M$. This effect is slightly more important when the value of $v_{COOH} = 55$ ml/mole than for $v_{COOH} = 59.3$ ml/mole.

The variations *versus* α of I^* normalized to K_x^2 and c_p are given in Fig. 11*a*, and a plateau is obtained above the Manning threshold, as expected. However, in a logarithmic representation, a discontinuity appears in the α range corresponding to the transition (Fig. 11*b*).

On the other hand, by using the same method of calculation, we found a continuous decrease of the contrast factor in neutron scattering, $K^2_{neutron}$, with α. For α equal to 0, 0.36 and 1, $K^2_{neutron} = 1.41*10^{-23}$ cm^2, $2.23*10^{-23}$ cm^2, $0.24*10^{-23}$ cm^2, respectively. This explains the differences in behaviours in X-rays and neutron scattering observed by Plestil et al. [43,44] well.

Finally, Fig. 12 gives some scattering results in the Kratky representation. While for the uncharged PMA, the $q^2 I(q)$ is a decreasing function of q after the maximum, an increase of this function is observed at high q values when $\alpha > 0.15$. It should be tempting to attribute such an evolution to a rigidification of the chain due to repulsive electrostatic interactions. Nevertheless, it is difficult to draw definitive conclusions on the changes in the local chain conformation, because the contribution of the structure factor in this q range is not known.

3.2.4.2. Influence of the concentration. Fig. 13 gives examples of scattering curves obtained by keeping α constant and varying c_p. The shift of the peak when c_p increases can be adjusted by the following power laws, according to the α value:

$$\alpha' = 0.09\ q* \approx c_p^{0.31} \tag{33}$$

$$\alpha' = 0.20\ q* \approx c_p^{0.36} \tag{34}$$

$$\alpha' = 0.95\ q* \approx c_p^{0.43} \tag{35}$$

For the lower value of α, the exponent is close to that expected for the dilute regime and the model of cubic lattice, a result consistent with our evaluation of c_p**. In such a model, the q^* values may be calculated from this simple expression, independent of α:

$$q* = \frac{2\pi}{\sqrt[3]{\dfrac{M_N}{c_p N_{av} 10^{-24}}}} \tag{36}$$

This leads to $q^* = 0{,}13 c_p^{1/3}$ in rather good agreement with the experimental law obtained for $\alpha' = 0.09$: $q^* = 0.16\ c_p^{0,31}$.

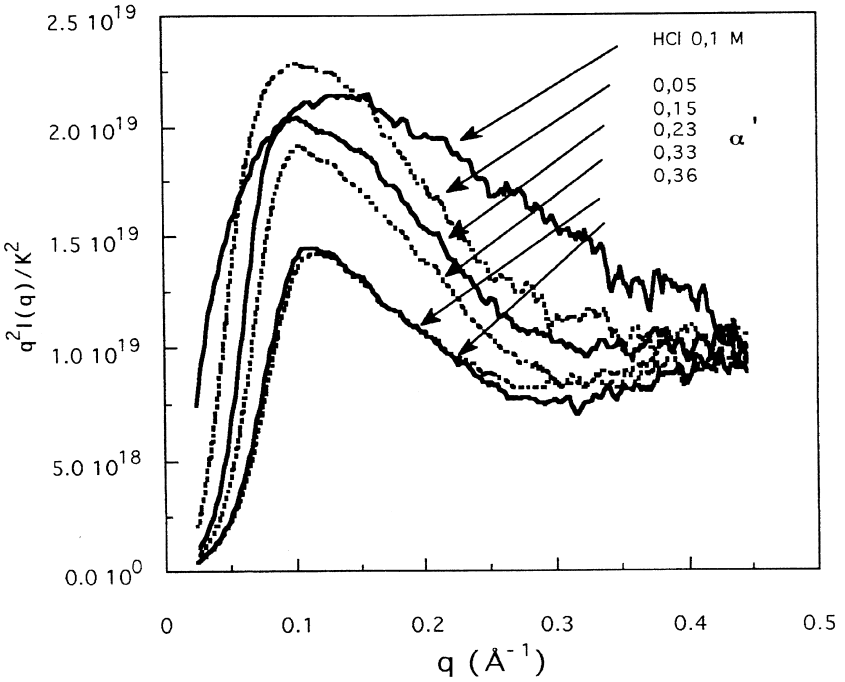

Fig. 12. X-ray scattering experiments on PMA in pure water: Kratky representation of the scattered intensity for different values of α.

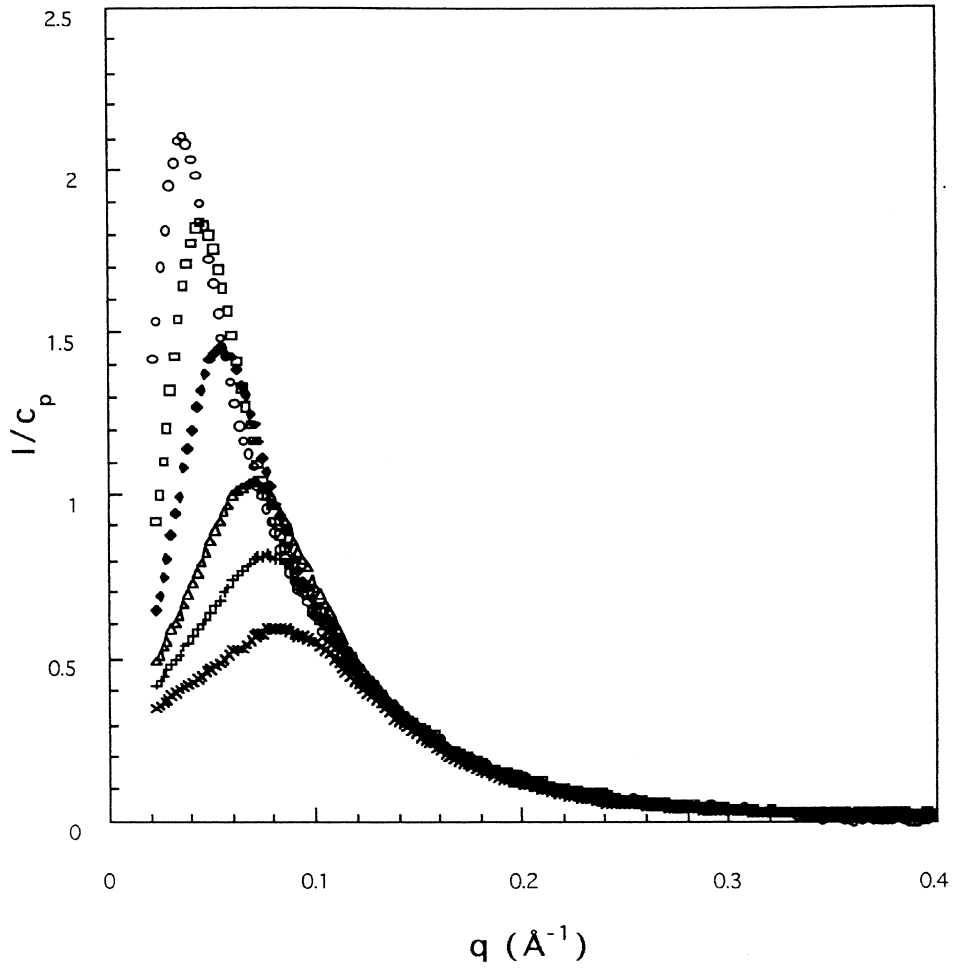

Fig. 13. X-ray scattering experiments on PMA in pure water: $\alpha = 0.09$ g/ml for different values of c_p (g/ml): $c_p = 0.0091$ (o), $c_p = 0.018$ (□), $c_p = 0.032$ (♦), $c_p = 0.065$ (△), $c_p = 0.098$ (+), $c_p = 0.14$ (x)

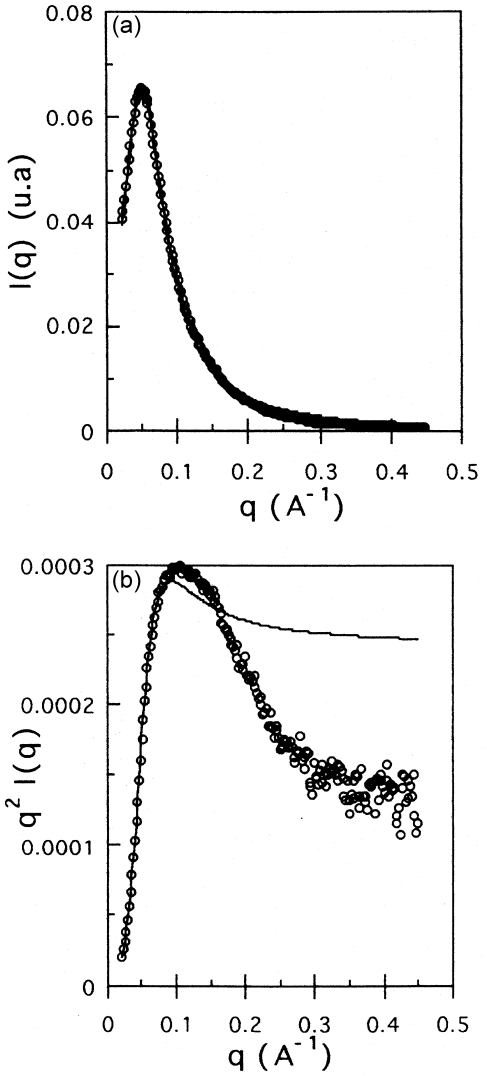

Fig. 14. X-ray scattering experiments on PMA in pure water. Example of fit of the scattering curves by relation (21): $c_p = 0.045$ g/ml, $\alpha = 0.05$: (a) $I(q) = f(q)$ representation, (b) Kratky representation

The exponent increases with α, indicating that the coil expansion induces the interpenetration of the chains. For $\alpha = 0.95$, the semi-dilute regime is reached and therefore the theoretical exponent 0.5 is almost obtained.

3.2.4.3. Discussion. Our results seem to be consistent with previous finding of Kaji et al. [22], or Boudenne and François [24], who have clearly shown the occurrence of concentration, molecular weight or charge parameter cross-overs between the dilute and semi-dilute regimes. This set of experimental results confirms, in terms of scaling laws, the behaviours predicted by the de Gennes et al. [26] and Pfeuty [28] theories.

Nevertheless, due to its hydrophobic character, PMA was often considered as a poor solvent in water, and it appeared as a good model to check the predictions of the mean field approach. Moossaid et al. [46,47] were able to adjust their experimental results obtained in the weak coupling limit

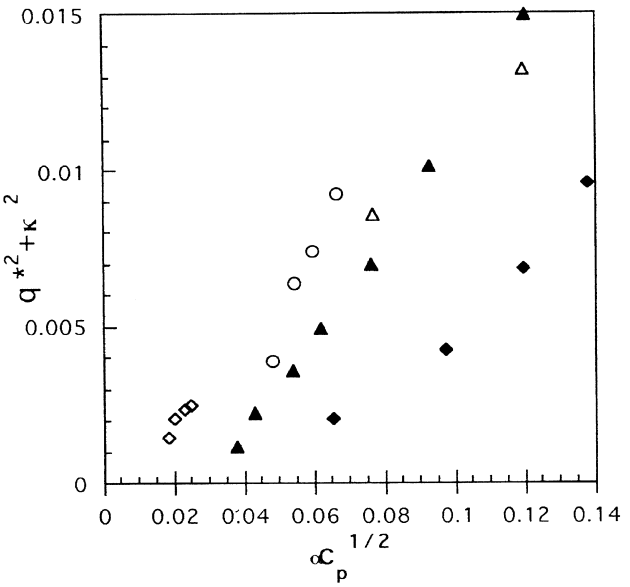

Fig. 15. Variation of $q^2 + \kappa^2$ *versus* $\alpha c_p^{1/2}$ for various α values $\alpha = 0.09$ (▲), $\alpha = 0.20$ (◆) [this work], $\alpha = 0.05$ (o), $\alpha = 0.02$ (◇), $\alpha = 0.109$ (△) [46,47]

(low α value) by the expression (21), considering three adjustable parameters: the contrast factor, the non-electrostatic viriel and the length of the statistical segment. Fig. 14 *a*, *b* show that by using the same method, the comparison between the calculated and experimental curves seems good in the $I(q) = f(q)$ representation, but the curves diverge significantly in the high q range in the Kratky representation. This confirms that the form factor of a weakly charged PMA is different from that of a gaussian coil. Besides, the K_x^2 value given by the fits was found to be four times higher than the calculated one. Finally, expression (21) implies the following variation of $q^{*2} + \kappa^2$

$$q^{*2} + \kappa^2 = \left[\frac{48\pi l_b}{b^2}\right]^{0.5} \alpha c_p^{0.5} \tag{37}$$

In Fig. 15, we have reported the variations $q^{*2} + \kappa^2$ versus $\alpha c_p^{0.5}$, as obtained in this work, and in that of Moussaid et al. [46,47]. It seems difficult to gather all the results corresponding to different α values on the same straight line. However, the two sets of data are in excellent agreement. This suggests that, in this range of concentrations and even at low ionization of the polymer, the mean field approximation cannot give a good account of the scattering results. Much more concentrated solutions have to be studied to verify these predictions.

4. Conclusion

The poly(methacrylic acid) exhibits a conformational transition. Although the nature of the compact conformation was not completely elucidated, this X-ray study suggests

that the uncharged PMA has overall dimensions intermediate between those of a compact sphere without water molecules inside it and a gaussian coil with a statistical segment close to that of other vinyl polymers. Portions of helices may give the best account for the high q behaviour of the scattering curves, and this may be due to syndiotactic sequences. A systematic study of the scattering behaviour as a function of the tacticity of the sample, completed by molecular modelling, should be useful to characterize the short distance conformation of the uncharged PMA.

When the ionization increases, the scattering functions exhibit a correlation peak whose position q^* has been systematically investigated *versus* the concentration and charge parameter. As far as the concentration dependence of q^* at a given ionization is concerned, one finds again that the results are consistent with the cubic lattice in the dilute regime and the isotropic model in the semi-dilute regime. The variation of q^* *versus* the ionization degree exhibits a discontinuity which is a manifestation of the conformational transition, and the results cannot be simply interpreted in the framework of the polyelectrolyte theories.

Acknowledgements

The authors would like to thank Dr Ph. Chaumont for preparing the PMA sample for this study. Mrs C. Bourgaux is also thanked for her help in the X-ray scattering experiments performed at the LURE laboratory in Orsay.

References

[1] Katchalsky A. J Polym Sci 1951;7:393.
[2] Arnold R, Overbeek J Th. Rec Trav Chim 1950;69:192.
[3] Leyte JC, Mandel M. J Polym Sci 1879;A2:1964.
[4] Liquori AM, Barone G, Crescenzi V, Quadrifoglio F, Vitagliano V. J. Macromol Chem 1966;1:291.
[5] Crescenzi V. Adv Polym Sci 1968;5:5388.
[6] Katchalsky A, Eisenberg H. J Polym Sci 1951;6:145.
[7] Noda I, Tsuge T, Nagasawa M. J Phys Chem 1970;74:710.
[8] Barone G, Crescenzi V, Pispisa B, Quadrifoglio F. J Macromol Chem 1966;1:761.
[9] Barone G, Crescenzi V, Liquori AM, Quadrifoglio F. J Phys Chem 1967;71:2341.
[10] Anufrieva EV, Birshtein TM, Nekrasova TN, Ptitsyn OB., Sheveleva TV. J Polym Sci C 1968;16:3519.
[11] Chen TS, Thomas JK. J Polym Sci 1979;17:1103.
[12] Olea AF, Thomas JK. Macromolecules 1989;22:1165.
[13] Delaire JA, Rodgers MAJ, Webber SE. J Phys Chem 1984;88:6219.
[14] Bednar B, Trnena J, Svoboda P. Macromolecules 1991;24:2054.
[15] Soutar I, Swanson L. Eur Polym J 1993;29:371.
[16] Crescenzi V, Quadrifoglio F, Delben F. J Polym Sci 1972;A2 (10):357.
[17] Skouri, Thesis, University Louis Pasteur, Strasbourg, 1994.
[18] Eliassaf J, Silberberg A. Polymer 1962;3:555.
[19] Drifford M, Dalbiez JP. J Phys Letters 1988;46:L–311.
[20] Nierlich M, Boué F, Oberthür R. J Phys France 1985;46:649.
[21] Williams CE, Nierlich M, Cotton JP, Jannink G, Boué F, Daoud M, Farnoux B, Picot C, de Gennes PG, Rinaudo M, Moan M, Wolff C. J Polym Sci, Polym Letters Ed 1979;17:379.
[22] Kaji K, Urakawa H, Kanaya T, Kitamaru R. J Phys France 1988;49:993.
[23] Xiao L, Reed WF. J Chem Phys 1991;94 (6):4568.
[24] Boudenne N, François J. Macromol Chem Phys 1995;196:3941.
[25] Förster S, Schmidt M, Antonietti M. Polymer 1990;31:781.
[26] de Gennes PG, Pincus P, Velasco RM, Brochard F. J Phys (Paris) 1976;37:1461.
[27] Odijk T. Macromolécules 1979;12:688.
[28] Pfeuty P. J Phys (Paris) 1978;C2:149.
[29] Borue V, Erukhimovitch I. Macromolecules 1988;21:3240.
[30] Joanny JF, Leibler L. J Phys France 1990;51:545.
[31] Hara M, Nakajima A. Polymer J 1980;12:711.
[32] Lin SC, Lee WI, Schurr JM. Biopolymers 1985;17:1041.
[33] Nicolai T, Mandel M. Macromolecules 1989;22:2348.
[34] Reed WF, Ghosh S, Medjadi G, François J. Macromolecules 1991;24:6189.
[35] Sedlak M, Konak C, Stepanek P, Jakes J. Polymer 1987;28:873.
[36] Sedlak M. Macromolecules 1993;26:1158.
[37] Moan M, Wolff C, Ober R. Polymer 1975;16:781.
[38] Moan M, Wolff C, Cotton JP, Ober R. J Polym Sci 1977;61:1.
[39] Moan M. J Appl Cryst 1978;11:519.
[40] Plestil J, Ostanevitch YM, Bezzabotonov VY, Hlavata D, Labsky J. Polymer 1986;27:839.
[41] Plestil J, Hlavata D, Labsky J, Ostanevitch YM, Bezzabotonov VY. Polymer 1987;28:213.
[42] Plestil J., Mikes J., Dusek K. Acta Polymerica 1979;30:29.
[43] Plestil J, Mikes J, Dusek K, Ostanevitch YM, Kunchenko AB. Polymer Bulletin 1981;4:225.
[44] Plestil J, Ostanevitch YM, Bezzabotonov VY, Hlavata D. Polymer 1986;27:1241.
[45] Muroga Y, Noda I, Nagasawa M. Macromolecules 1985;18:1580.
[46] Moussaid A, Schossler F, Munch JP, Candau SJ. J Phys II France 1993;3:573.
[47] A Moussaid, Thèse, Strasbourg, 1994.
[48] Blumstein R, Murphy G, Blumstein A, Watterson AC. Polym Letters 1973;11:21.
[49] C Schloesser-Becker, Thèse, Université Louis Pasteur, Strasbourg, 1991.
[50] Greschner GS. Makromol. Chem 1973;170:203.
[51] Tondre C, Zana R. J Phys Chem 1972;76:23.
[52] Kanda A, Duval M, Sarazin D, François J. Polymer 1985;26:406.
[53] Rawiso M, Duplessix R, Picot C. Macromolecules 1987;20:630.
[54] Rawiso M, Aime JP, Fave JL, Scott M, Müller MA, Schmidt M, Baumgartll H, Wegner G. J Phys France 1988;49:861.
[55] Dobrymin AV, Colby RH, Rubinstein M. Macromolecules 1995; 28: 1859.
[56] Kirste RG. Makromol Chem 1967;101:91.
[57] Kirste RG. J Polym Sci Part C 1967;16:2039.
[58] Mandel M. Eur Polym J 1970;6:807.
[59] El Brahmi K, Rawiso M, François J. Eur Polym J 1993;29:1531.
[60] Overbeek J Th. Bull Soc Chim Belg 1948;57:252.
[61] Hermans JJ, Overbeek J Th. Bull Soc Chim Belg 1948;57:154.
[62] Katchalsky A, Shavit N, Eisenberg H. J Polym Sci 1954;13:69.
[63] Kotin L, Nagasawa N. J Chem Phys 1962;84:873.
[64] Lifson S, Katchalsky A. J Polym Sci 1954;13:43.
[65] Nagasawa M, Murase T, Kondo K. J Phys Chem 1965;69:4005.
[66] C Heitz, Thesis, Louis Pasteur University, Strasbourg, 1996.
[67] Manning GS. J Chem Phys 1969;5:924.
[68] Yamashita F, Kwak JT. J Pol Sci Part B 1987;25:1395.